American Mineralogist, Volume 106, pages 1917–1927, 2021

Keplerite, $Ca_9(Ca_{0.5}\square_{0.5})Mg(PO_4)_7$, a new meteoritic and terrestrial phosphate isomorphous with merrillite, $Ca_9NaMg(PO_4)_7$

Sergey N. Britvin[1,2,*], Irina O. Galuskina[3], Natalia S. Vlasenko[4], Oleg S. Vereshchagin[1,†], Vladimir N. Bocharov[4], Maria G. Krzhizhanovskaya[1], Vladimir V. Shilovskikh[4,5,‡], Evgeny V. Galuskin[3], Yevgeny Vapnik[6], and Edita V. Obolonskaya[7]

[1]Institue of Earth Sciences, St. Petersburg State University, Universitetskaya Nab. 7/9, 199034 St. Petersburg, Russia
[2]Kola Science Center, Russian Academy of Sciences, Fersman Str. 14, 184209 Apatity, Russia
[3]Faculty of Natural Sciences, Institute of Earth Sciences, University of Silesia, Bedzińska 60, 41-200 Sosnowiec, Poland
[4]Centre for Geo-Environmental Research and Modelling, St. Petersburg State University, Ulyanovskaya str. 1, 198504 St. Petersburg, Russia
[5]Institute of Mineralogy, Urals Branch of Russian Academy of Science, Miass 456317, Russia
[6]Department of Geological and Environmental Sciences, Ben-Gurion University of the Negev, POB 653, Beer-Sheva 84105, Israel
[7]The Mining Museum, St. Petersburg Mining University, 2, 21st Line, 199106 St. Petersburg, Russia

Abstract

Keplerite is a new mineral, the Ca-dominant counterpart of the most abundant meteoritic phosphate, which is merrillite. The isomorphous series merrillite-keplerite, $Ca_9NaMg(PO_4)_7$-$Ca_9(Ca_{0.5}\square_{0.5})Mg(PO_4)_7$, represents the main reservoir of phosphate phosphorus in the solar system. Both minerals are related by the heterovalent substitution at the *B*-site of the crystal structure: $2Na^+$ (merrillite) → $Ca^{2+} + \square$ (keplerite). The near-end-member keplerite of meteoritic origin occurs in the main-group pallasites and angrites. The detailed description of the mineral is made based on the Na-free type material from the Marjalahti meteorite (the main group pallasite). Terrestrial keplerite was discovered in the pyrometamorphic rocks of the Hatrurim Basin in the northern part of Negev desert, Israel. Keplerite grains in Marjalahti have an ovoidal to cloudy shape and reach 50 μm in size. The mineral is colorless, transparent with a vitreous luster. Cleavage was not observed. In transmitted light, keplerite is colorless and non-pleochroic. Uniaxial (−), ω = 1.622(1), ε = 1.619(1). Chemical composition (electron microprobe, wt%): CaO 48.84; MgO 3.90; FeO 1.33; P_2O_5 46.34, total 100.34. The empirical formula (O = 28 apfu) is $Ca_{9.00}(Ca_{0.33}Fe^{2+}_{0.20}\square_{0.47})_{1.00}Mg_{1.04}P_{6.97}O_{28}$. The ideal formula is $Ca_9(Ca_{0.5}\square_{0.5})Mg(PO_4)_7$. Keplerite is trigonal, space group *R*3*c*, unit-cell parameters refined from single-crystal data are: a = 10.3330(4), c = 37.0668(24) Å, V = 3427.4(3) Å^3, Z = 6. The calculated density is 3.122 g/cm^{-3}. The crystal structure has been solved and refined to R_1 = 0.039 based on 1577 unique observed reflections [$I>2\sigma(I)$]. A characteristic structural feature of keplerite is a partial (half-vacant) occupancy of the sixfold-coordinated *B*-site (denoted as CaIIA in the earlier works). The disorder caused by this cation vacancy is the most likely reason for the visually resolved splitting of the ν_1 (symmetric stretching) (PO_4) vibration mode in the Raman spectrum of keplerite. The mineral is an indicator of high-temperature environments characterized by extreme depletion of Na. The association of keplerite with "*REE*-merrillite" and stanfieldite provides evidence for the similarity of temperature conditions that occurred in the Mottled Zone to those expected during the formation of pallasite meteorites and lunar rocks. Because of the cosmochemical significance of the merrillite-keplerite series and by analogy to plagioclases, the Na-number measure, 100×Na/(Na+Ca) (apfu), is herein proposed for the characterization of solid solutions between merrillite and keplerite. The merrillite end-member, $Ca_9NaMg(PO_4)_7$, has the Na-number = 10, whereas keplerite, $Ca_9(Ca_{0.5}\square_{0.5})Mg(PO_4)_7$, has Na-number = 0. Keplerite (IMA 2019-108) is named in honor of Johannes Kepler (1571–1630), a prominent German naturalist, for his contributions to astronomy and crystallography.

Keywords: Keplerite, merrillite, whitlockite, phosphate, meteorite, pallasite, angrite, pyrometamorphism

Introduction

The whitlockite mineral group incorporates eight natural phosphates whose general chemical formula can be expressed as $A_9BM(PO_3X)_4(PO_4)_3$, where the species-defining constituents A = Ca or Sr; B = Na, Ca or □ (vacancy); M = Mg, Fe^{2+}, or Mn^{2+}; and X is either O or OH (Table 1). Among these minerals, two species are of particular importance in biochemistry and planetary science. The water-containing whitlockite, $Ca_9Mg(PO_3OH)(PO_4)_6$, is a very rare terrestrial phosphate (Frondel 1941, 1943) but a common constituent of all vertebrates' bone tissues (Wang and Nancollas 2008). The anhydrous species, merrillite, $Ca_9NaMg(PO_4)_7$, the first discovered whitlockite-group mineral

* E-mail: sergei.britvin@spbu.ru
† Orcid 0000-0002-4811-2269
‡ Orcid 0000-0003-2326-700X

0003-004X/21/0012–1917$05.00/DOI: https://doi.org/10.2138/am-2021-7834

Table 1. Whitlockite-group minerals approved by CNMNC IMA[a]

Mineral[b]	Ideal formula	Species-defining constituents			
		A	B	M	X
	Anhydrous members				
Merrillite [2]	$Ca_9NaMg(PO_4)_7$	Ca	Na	Mg	O
Keplerite [1]	$Ca_9(Ca_{0.5}\square_{0.5})Mg(PO_4)_7$	Ca	$Ca_{0.5}\square_{0.5}$	Mg	O
Ferromerrillite [3]	$Ca_9NaFe^{2+}(PO_4)_7$	Ca	Na	Fe^{2+}	O
Matyhite [4]	$Ca_9(Ca_{0.5}\square_{0.5})Fe^{2+}(PO_4)_7$	Ca	$Ca_{0.5}\square_{0.5}$	Fe^{2+}	O
	Hydrogen-bearing members				
Whitlockite [5]	$Ca_9Mg(PO_3OH)(PO_4)_6$	Ca	□	Mg	OH
Strontiowhitlockite [6]	$Sr_9Mg(PO_3OH)(PO_4)_6$	Sr	□	Mg	OH
Wopmayite [7]	$Ca_6Na_3\square Mn^{2+}(PO_4)_3(PO_3OH)_4$	Ca	□	Mn^{2+}	OH
Hedegaardite [8][c]	$(Ca,Na)_9(Ca,Na)Mg(PO_3OH)(PO_4)_6$				

[a] Commission on New Minerals, Nomenclature and Classification of the International Mineralogical Association.
[b] References: [1] this work; [2] Xie et al. (2015); [3] Britvin et al. (2016); [4] Hwang et al. (2019); [5] Calvo and Gopal (1975); [6] Britvin et al. (1991); [7] Cooper et al. (2013); [8] Witzke et al. (2015).
[c] Crystal structure of hedegaardite was not published.

(Merrill 1915), is the most abundant meteoritic phosphate, a dominant carrier of phosphate phosphorus in the cosmic matter. Merrillite is a common accessory phase of ordinary chondrites (Fuchs 1962; Van Schmus and Ribbe 1969; Jones et al. 2014, 2016; Lewis and Jones 2016); it occurs in carbonaceous chondrites, many groups of achondrites, stony-iron, and iron meteorites (Buseck and Holdsworth 1977; Ward et al. 2017) in lunar rocks and martian meteorites (Jolliff et al. 2006; Shearer et al. 2015). It is considered to be the primary phosphate phase formed during protoplanetary nebula condensation (Pasek 2015). Merrillite forms a continuous series of solid solutions with its Fe^{2+}-dominant analog, ferromerrillite, $Ca_9NaFe(PO_4)_7$—a phosphate typical of martian shergottites (Britvin et al. 2016). Terrestrial merrillite was discovered in mantle xenoliths from Siberia, Russia (Ionov et al. 2006) and was recently encountered in phosphate assemblages of pyrometamorphic rocks belonging to the Hatrurim Formation, Israel (Galuskina et al. 2016). Merrillite has three notable chemical features. First, this is a water-free mineral, in contrast to a majority of terrestrial whitlockite-group members, which bear water as a constituent of hydrogen phosphate groups (Table 1). Second, merrillite is devoid of F and Cl. Last, the mineral contains an appreciable amount of Na. The two latter features highlight the differences between merrillite and another abundant meteoritic phosphate—apatite (McCubbin and Jones 2015; Ward et al. 2017). Merrillite is an important reservoir for meteoritic Na. The mineral tends to accumulate even the traces of Na available in the mineral system (e.g., Buseck and Holdsworth 1977). However, upon complete lack of this element in the environment, the only way to maintain the charge balance and structure of merrillite is to compensate Na by other elements. The prime candidates for such a replacement are Ca and *REE* (e.g., Jolliff et al. 2006; Hughes et al. 2006).

There are two meteorite groups whose members are extremely depleted in Na—these are the pallasites and angrites. Pallasites are the stony-iron meteorites considered as products of fractional melting of chondrite parent body (Boesenberg et al. 2012). Angrites have basaltic composition and textures, and they are the most alkali-depleted basalts in the solar system (Keil 2012). It is thus not surprising that the first finding of Ca-dominant analog of merrillite was confined to the angrite meteorite, Angra dos Reis (Dowty 1977). In the same year, Buseck and Holdsworth (1977) published a detailed report on phosphate mineral assemblages in pallasites, where they identified a similar Na-depleted Ca-phosphate. At that time, meteoritic merrillite was not definitely recognized as an analog of whitlockite: the crystal structure of natural merrillite, $Ca_9NaMg(PO_4)_6$, was determined much later (Xie et al. 2015; Britvin et al. 2016). The absence of knowledge regarding the relationships between merrillite and whitlockite has led to ambiguities in the naming of these minerals (see Adcock et al. 2014). Because of that, both Dowty (1977) and Buseck and Holdsworth (1977) ascribed the reported mineral to whitlockite, whose formula was at that time accepted as $Ca_3(PO_4)_2$, by analogy to synthetic β-$Ca_3(PO_4)_2$ (Frondel 1941).

Although the mineral from Angra dos Reis (Dowty 1977) is essentially enriched in Ca, it still contains a noticeable amount of Na (Keil et al. 1976) (Table 2). However, a survey of analyses reported by Buseck and Holdsworth (1977) reveals "whitlockite" having considerably lower Na_2O content, down to the Na-free phosphate occurring in the Marjalahti and Ahumada pallasites (Table 2). We have determined the crystal structure of the latter mineral and found that it represents the Na-free counterpart of merrillite, previously known as a synthetic dehydrogenation product of whitlockite (Hughes et al. 2008; Adcock et al. 2014). Consequently, this is a new mineral species distinct from both merrillite and whitlockite (Table 1). In the course of ongoing research of the unusual pyrometamorphic complex, the Hatrurim Formation (the Mottled Zone) in the Southern Levant, the same mineral has been confirmed in the Hatrurim Basin, Negev desert, Israel. Therefore, this Na-depleted analog of merrillite is currently recognized as both a meteoritic and terrestrial species. The new mineral was named keplerite, in honor of Johannes Kepler (1571–1630), a prominent German scientist, for his contributions to astronomy and crystallography (e.g., Kepler 1611). Both the mineral and the name have been approved by the Commission on New Minerals, Nomenclature and Classification of the Interna-

Table 2. Chemical composition of meteoritic keplerite

Meteorite	Marjalahti		Angra dos Reis	Ahumada	Imilac	Somervell County	Lew 86010
Group	Pallasite		Angrite	Pallasite	Pallasite	Pallasite	Angrite
Reference[a]	[1]	[2]	[3]	[2]	[2]	[2]	[4]
				wt%[c]			
Na_2O	–	–	0.68	0.10	0.52	0.68	0.4
CaO	48.87	48.8	49.4	49.1	50.2	48.7	50.7
MgO	3.90	4.52	2.82	3.32	3.62	3.76	2.68
FeO	1.33	0.88	1.29	1.85	0.36	0.50	1.62
P_2O_5	46.24	45.2	45.1	45.6	45.9	46.8	44.6
SiO_2	–	–	0.67	0.32	–	0.08	0.68
Total	100.34	99.40	99.96	100.29	100.60	100.52	100.7
				Formula amounts (O = 28 apfu)			
Na	–	–	0.24	0.03	0.18	0.23	0.14
Ca	9.33	9.42	9.52	9.42	9.58	9.24	9.76
Σ(Ca,Na)	9.33	9.42	9.76	9.45	9.76	9.48	9.90
Mg	1.04	1.21	0.76	0.89	0.96	0.99	0.72
Fe^{2+}	0.20	0.13	0.19	0.28	0.05	0.07	0.24
Σ(Mg,Fe)	1.24	1.34	0.95	1.17	1.01	1.06	0.96
P	6.97	6.89	6.87	6.91	6.92	7.02	6.79
Si	–	–	0.12	0.06	–	0.01	0.12
Σ(P,Si)	6.97	6.89	6.99	6.97	6.92	7.03	6.91
Mg-number	84	90	80	76	94	93	75
Na-number	0	0	2.4	0.4	1.8	2.5	1.4

[a] References: [1] this work, holotype specimen; [2] Buseck and Holdsworth (1977); [3] Keil et al. (1976); [4] Crozaz and McKay (1990).
[b] Contains 0.03 wt% K_2O and 0.08 wt% MnO (0.01 K and Mn apfu).
[c] The dash means below detection limit.

tional Mineralogical Association (IMA 2019-108). The holotype specimen of keplerite from the Marjalahti pallasite is deposited in the collections of the Mining Museum, St. Petersburg Mining University, St. Petersburg, Russia, catalog number MM74/2-1.

Materials and methods

The pieces of the Marjalahti and the Brahin pallasites (MM74/2 and MM65/2, respectively) were kindly provided for this study by the curators of the Mining Museum, Saint Petersburg Mining University. The chip of the Los Angeles shergottite was obtained from Sergey Vasiliev (https://sv-meteorites.com/). The specimens containing terrestrial keplerite were collected by I.O.G., E.V.G., and Ye.V. during field trips.

Electron microprobe analyses (EMPA) and SEM study of meteoritic keplerite and associated minerals were carried out on the polished carbon-coated sections by means of a Hitachi S-3400N SEM with an attached INCA WAVE 500 WDX spectrometer (20 kV, 10 nA), using the following standards and lines: chlorapatite (Ca*Kα*, P*Kα*); diopside (Mg*Kα*); and hematite (Fe*Kα*). A complete set of chemical analyses of holotype keplerite from the Marjalahti meteorite is given in Online Materials[1] Table OM1. The chemical composition of terrestrial keplerite and associated minerals was studied by means of a CAMECA SX100 WDX analyzer (15 kV, 20 nA) using the following standards and lines: fluorapatite (P*Kα*, F*Kα*); diopside (Mg*Kα*, Ca*Kα*, Si*Kα*); orthoclase (Al*Kα*, K*Kα*); hematite (Fe*Kα*); rhodochrosite (Mn*Kα*); albite (Na*Kα*); baryte (Ba*Lα*, S*Kα*); celestine (Sr*Lα*); V_2O_5 (V*Kα*); YPO_4 (Y*Lα*); La-glass-Geochr (La*Lα*); CeP_5O_{11} (Ce*Lα*); SmP_5O_{11} (Sm*Lβ*); $NdGeO_3$ (Nd*Lβ*); Pr-glass-Geochr (Pr*Lβ*).

X-ray single-crystal study of the type keplerite crystal was performed based on the data collected with a Bruker Kappa APEX DUO diffractometer equipped with a microfocus Mo*Kα*-radiation source and 1024K APEXII CCD detector. Data collection and unit cell refinement were performed using a built-in Bruker APEX2 program package, whereas integration procedures were carried out with a CrysAlisPro software (Rigaku Oxford Diffraction 2018). Crystal structure solution and refinement were carried out with the *hkl* data set truncated at $2\Theta = 54°$, using a SHELX-2018 program suite incorporated into the Olex2 operational environment (Sheldrick 2015; Dolomanov et al. 2009). The complete set of data collection and structure refinement details can be retrieved from the Crystallographic Information File (CIF) attached to the Online Materials[1]. A brief summary of data collection and refinement parameters is given in Online Materials[1] Table OM2.

The powder X-ray diffraction pattern of holotype keplerite was calculated on the basis of structural data (Online Materials[1] Table OM3). An optical study was performed using a Leica DM 4500 P polarizing microscope and a standard set of immersion liquids. The metal sections intended for the study in reflected light were etched with nital solution (2 parts of 65% HNO_3 per 98 parts of ethanol). Raman spectra of meteoritic (holotype) keplerite were recorded with a Horiba Jobin-Yvon LabRam HR800 instrument equipped with an Ar-ion laser ($\lambda = 514$ nm), using an Olympus BX41 microscope through the 50× confocal objective. The spectral resolution was set to 2 cm^{-1}, acquisition time was 30 s, and each data set was averaged from 20 scans. The spectrometer was preliminary calibrated using the 520.7 cm^{-1} line of a silicon standard. Raman spectra of terrestrial keplerite were recorded on a WITec α 300 R Confocal Raman Microscope equipped with an air-cooled solid-state laser (532 nm) and 100× confocal objective. Integration times of 5 s with an accumulation of 20–30 scans and a resolution 2 cm^{-1} were chosen. The monochromator was calibrated using the Raman scattering line of a silicon plate (520.7 cm^{-1}).

Results

Occurrence, appearance, and properties

The Marjalahti pallasite (type locality). A few fragments of the ~45 kg Marjalahti mass were collected on June 1, 1902, shortly after the meteorite fall that hit the granite outcrop at Marjalahti bay, the northern coast of Lake Ladoga, Karelia, Russia. Being one of four witnessed pallasite falls (Grady 2000), Marjalahti was not affected by weathering. Like other main-group pallasites, the meteorite consists of centimeter-sized olivine crystals embedded into the α-(Fe,Ni) (kamacite) matrix. The α-(Fe,Ni) metal of the studied Marjalahti section contains 5.7 wt% Ni and 0.85 wt% Co; it is penetrated by a dense net of Neumann bands—the traces of shock-induced deformation twins revealed by nital etching (Fig. 1) (e.g., Uhlig 1955). Subordinate mineral phases of Marjalahti include chromite, troilite, schreibersite, nickelphosphide, tetrataenite, and trace amounts of nazarovite, $Ni_{12}P_5$ (IMA 2019-013). The Marjalahti phosphate, being recognized as merrillite, was a subject of research aimed at determining its fission track age (e.g., Pellas et al. 1983). However, there are no analytical data providing evidence for the occurrence of genuine merrilite, $Ca_9NaMg(PO_4)_7$ in this meteorite.

Keplerite in Marjalahti is confined to the specific troilite-orthopyroxene vermicular intergrowths (symplectites) developed along the contacts between olivine and Fe-Ni metal (Fig. 2). The assignment of pyroxene to the orhorhombic enstatite was made by the use of a single-crystal XRD analysis. Troilite in symplectites and in adjacent grains (Figs. 2a and 2b) has a perfect FeS stoichiometry and does not contain detectable Cr, V, or Ti impurities. It is noteworthy that troilite inclusions in contact with symplectites have pronounced outer rims composed of microgranular porous troilite. Keplerite occurs as chains of ovoidal to cloud-like inclusions in both olivine and orthopyroxene, at the peripheral zone of symplectites, immediately at the contact with (Fe,Ni) metal. The biggest grain encountered was ~40 μm in length. Keplerite is colorless, transparent with a vitreous luster, and shows no cleavage. It is non-fluorescent under long- and short-wavelength UV light. Examination in immersion liquids in transmitted light showed the mineral is colorless and non-pleochroic. It is uniaxial (−), $\omega = 1.622(1)$, $\varepsilon = 1.619(1)$. The Gladstone-Dale compatibility index (Mandarino 1981) is –0.010 (superior). The density calculated based on the empirical formula and the unit-cell volume refined from single-crystal X-ray diffraction data is 3.122 g/cm^{-3}.

The Hatrurim Basin. Being the largest complex of pyrometamorphic rocks in Israel, the Hatrurim Basin occupies an area of ~50 km^2 a few kilometers to the west of the southern subbasin of the Dead Sea. The Hatrurim Basin belongs to a pyrometamorphic suite known as the Hatrurim Formation or the Mottled Zone (e.g., Gross 1977; Burg et al. 1999; Vapnik et al. 2007; Geller et al. 2012; Novikov et al. 2013). The diverse

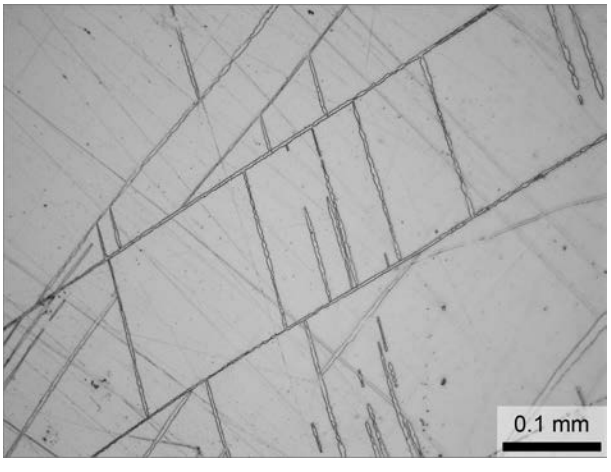

Figure 1. Neumann bands (shock-induced deformation twins) in the α-(Fe,Ni) metal matrix of the Marjalahti pallasite. Polished section after nital etching. Photomicrograph in reflected light.

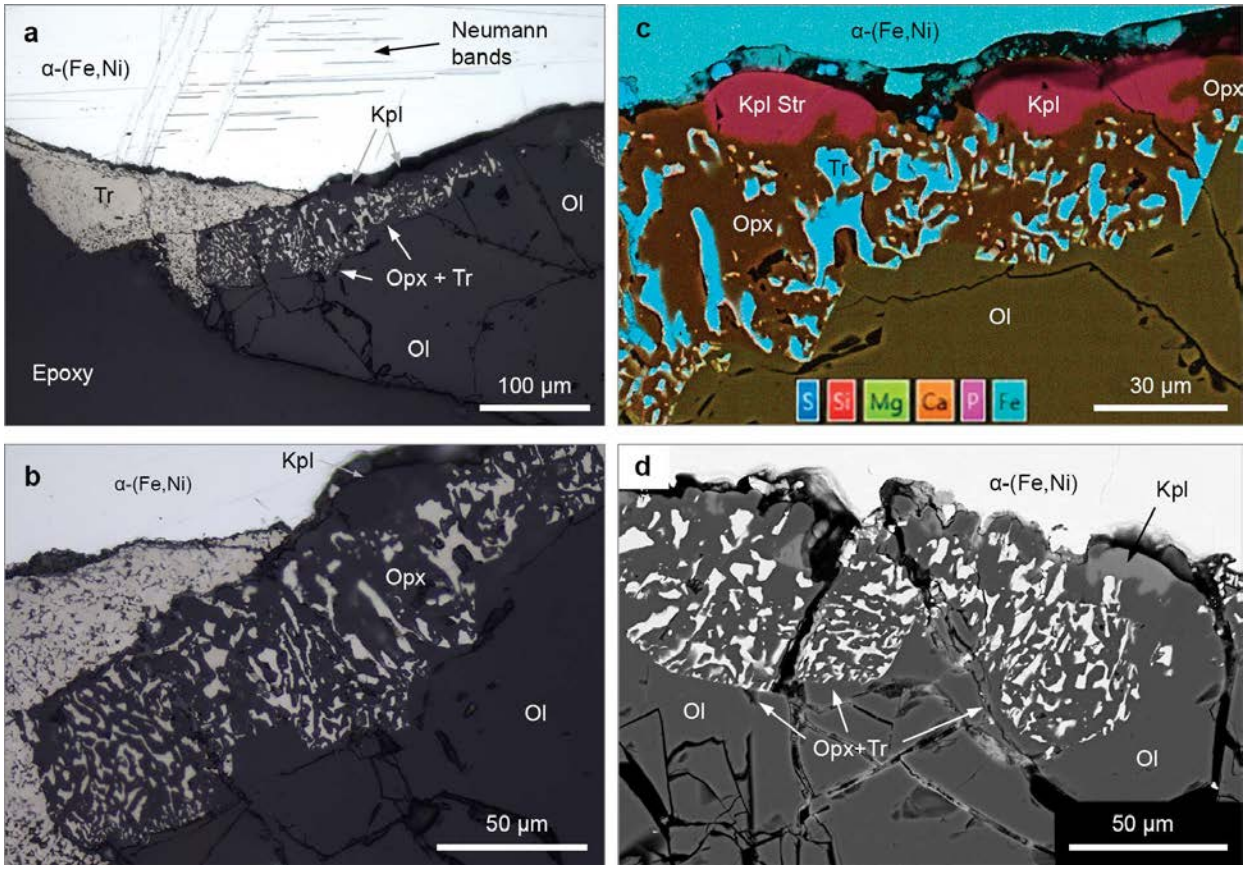

Figure 2. Keplerite-bearing assemblages in the Marjalahti pallasite. (**a**) Troilite-orthopyroxene symplectites with two keplerite inclusions along the contact of olivine and α-(Fe,Ni) metal. The Neumann bands penetrate the metal and abut against troilite. Reflected light. (**b**) Detail of the same fragment. Note the porous microgranular troilite texture at the contact with symplectite. Reflected light. (**c**) Detailed view of two keplerite inclusions depicted in **a**. False color EDX map in characteristic X-rays of respective elements. (**d**) SEM BSE image of keplerite inclusion embedded in olivine. Abbreviations: Kpl = keplerite; Tr = troilite; Ol = olivine; Opx = orthopyroxene. The keplerite grain marked as Kpl Str was used for X-ray structure determination. (Color online.)

mineralogy of the Hatrurim Formation gathers Earth's exotic and often genetically incompatible mineral assemblages produced by the superposition of several processes: (1) pyrometamorphism at temperatures reaching 1400 °C that has led to the calcination and fusion of sedimentary strata and was accompanied by the formation of paralavas and high-temperature alteration of the early "clinker" mineral associations; (2) post-metamorphic low-temperature hydrothermal activity; and (3) supergene alteration of high-temperature assemblages (Gross 1977; Galuskina et al. 2014; Britvin et al. 2015; Galuskin et al. 2016; Sokol et al. 2019; Khoury 2020). Keplerite is confined to the rocks belonging to the pyrometamorphic stage. The mineral was identified in the brecciated, altered pyroxene paralava (fused sediments) outcropping on the slope of a hill in the Negev Desert near the town of Arad (31°13′58″N; 35°16′2″E). (Fig. 3). The paralava forms an irregular rounded field of ~20 m across, within the area occupied by the gray and red spurrite marbles. The marbles in the vicinity of the reported locality are known for the diversity of exotic minerals, such as ariegilatite, stracherite, and aravaite (Galuskin et al. 2018a, 2018b; Krüger et al. 2018). Large blocks of brecciated paralava are color-zoned—from brick-red to gray in the central parts to olive-green at the periphery. The interiors of the blocks are filled with paralava fragments of two types, distinguished by the composition and color. The first type is comprised of fine-grained gray angular chunks (Fig. 4a) composed of diopside [mean composition $(Ca_{0.94}Na_{0.06})(Mg_{0.82}Fe^{3+}_{0.11}Al_{0.07})(Si_{1.88}Al_{0.12})O_6$], subordinate wollastonite, andradite, and rare anorthite. The red rims enclosing the gray fragments are colored by finely dispersed hematite (Fig. 4b). The rock fragments of the second type have a yellow-green color (Fig. 4a); they fill the interstices between the gray fragments. The yellow-green rocks consist of fine grains of diopside-esseneite pyroxene [mean composition $Ca(Mg_{0.7}Fe^{3+}_{0.2}Al_{0.1})(Si_{1.7}Al_{0.3})O_6$], wollastonite, and fluorapatite, which are dispersed within a matrix of secondary zeolites, Ca-hydrosilicates, hydrogarnets, and calcite. The diopside-esseneite grains are commonly outlined by the thin zones of aegirine [mean composition $(Na_{0.59}Ca_{0.41})(Fe^{3+}_{0.57}Mg_{0.31}Fe^{2+}_{0.10}Al_{0.01})Si_2O_6$]. The rock fragments of both types are cemented and penetrated by a white-colored suite of the late minerals, including baryte, calcite, zeolites, tacharanite, afwillite, and tobermorite-group silicates (Figs. 4a and 4b). Hematite nodules that reach several centimeters in size are the specific feature of the reported paralava. Besides of the dominant hematite, the nodules contain magnesioferrite, maghemite, ilmenite, pseudobrookite, hibonite, dorrite, and

kahlenbergite, $KAlFe_{10}O_{17}$ (Krüger et al. 2019). The minerals related to the join merrillite-keplerite occur as the aggregates up to 0.2 mm in size scattered within the fine-grained gray paralava; they are often intergrown with fluorapatite and likely replace the latter (Figs. 4c–4e; Table 3). Monazite and xenotime inclusions are observed in those fluorapatite crystals that are not intergrown with keplerite (Fig. 4f). A merrillite-like mineral with anomalously high-*REE* content, (Ca,*REE*)$Mg(PO_4)_7$, and stanfieldite are rarely encountered in the same association (Fig. 4e; Table 3).

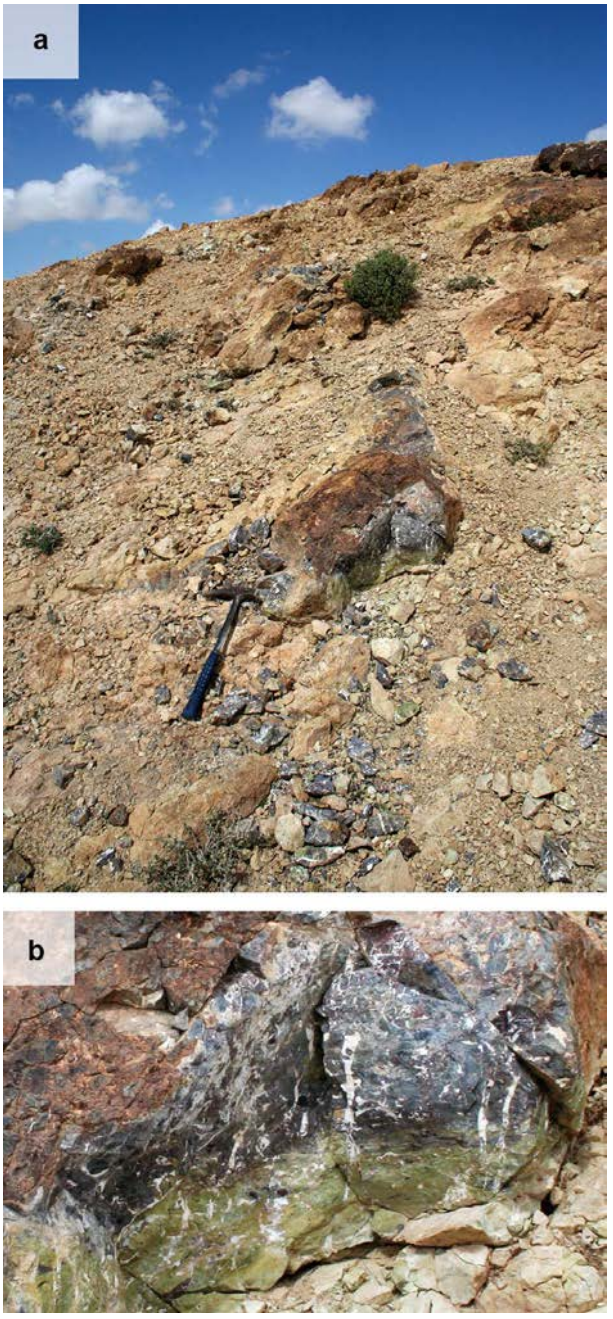

Figure 3. Keplerite-bearing pyrometamorphic paralavas of the Hatrurim Basin, Negev desert, Israel. (**a**) The outcrop of the paralava on the hill. (**b**) A close view of the paralava. (Color online.)

This is the first terrestrial occurrence of *REE*-bearing merrillite-group mineral and stanfieldite, both previously known only in lunar rocks and meteorites (Jolliff et al. 2006; Britvin et al. 2020).

Chemical composition

The summary of the chemical data on meteoritic keplerite is provided in Table 2; the data on terrestrial keplerite are given in Table 3. The characteristic feature of terrestrial keplerite, distinguishing it from the meteoritic one, is the presence of *REE* and the low-iron content. One can see that the majority of keplerite analyses, including those for the mineral from Angra dos Reis (Keil et al. 1976; Dowty 1977) show noticeable concentrations of Na and hence represent the intermediate members of solid solutions between keplerite and merrillite. Keplerite from Marjalahti (and Ahumada) is unique in this respect as it does not contain Na. Besides, there are two chemical features of the Marjalahti mineral, which are directly related to its origin and crystal structure. The orthopyroxene ($En_{0.88}Fs_{0.12}$) in keplerite-containing symplectites (Fig. 2) and adjacent olivine ($Fo_{0.88}Fa_{0.12}$) have the same Mg-number [100×Mg/(Mg+Fe)] equal to 88 (Online Materials[1] Table OM4). The Mg-number of keplerite is 83—the mineral is obviously enriched in Fe relative to both coexisting silicates. The empirical formula of the type Marjalahti keplerite, calculated on the basis of 28 oxygen atoms per formula unit (apfu), is $Ca_{9.00}(Ca_{0.33}Fe^{2+}_{0.20}\square_{0.47})_{1.00}Mg_{1.04}P_{6.97}O_{28.00}$. Therefore, the sum of *M*-site cations, i.e., (Mg+Fe), is equal to 1.24 apfu that is considerably higher than the unity dictated by the ideal keplerite stoichiometry, $Ca_9(Ca_{0.5}\square_{0.5})Mg(PO_4)_7$. The substantial excess of (Mg+Fe) was previously reported for the mineral from Marjalahti and for keplerite of the same, "symplectic" origin from the Ahumada pallasite (Table 2) (Buseck and Holdsworth 1977). At the same time, keplerite and merrillite of non-symplectic origin and terrestrial mineral do not exhibit (Mg+Fe) excess. Therefore, the observed "extra" contents of octahedral cations in keplerite from symplectites are not an artifact and thus require explanation, which is given below.

Crystal structure

The basic features of keplerite structure are the same as of other whitlockite-group minerals whose general structural formula can be expressed as $[A(1)_3\,A(2)_3\,A(3)_3]\,B\,M\,[P(1)\,P(2)_3\,P(3)_3]\,O_{24}\,X_4$, leading to a chemical formula $A_9BM(PO_3X)_4(PO_4)_3$ (Table 1). The whitlockite-type framework consists of an arrangement of $[PO_4]$ tetrahedra and cation-centered polyhedra $[AO_8]$, $[BO_6]$, and $[MO_6]$ linked via the common corners and edges, forming a series of rods propagated along the *c*-axis (Gopal and Calvo 1972; Moore 1973). The arrangement of species-defining $[BO_6]$ and $[MO_6]$ polyhedra is shown in Figure 5. The $[MO_6]$ unit in the whitlockite structure type is a slightly distorted octahedron readily incorporating Mg^{2+}, Fe^{2+}, or Mn^{2+} (Table 1). There are no references evident for the possibility of vacancies at the *M*-site. The free refinement of the *M*-site population in the type keplerite from the Marjalahti pallasite shows that this position is occupied solely by Mg^{2+}, consistent with the equality of *M*-O bond lengths in the Marjalahti keplerite and classic merrillite having near-zero Fe contents (Table 4). In contrast, the *M*-O bond lengths in the mineral from Angra dos Reis (Dowty 1977) are noticeably longer, in accordance with the higher Fe^{2+} population at the *M*-site (Table 4). Therefore, considering that

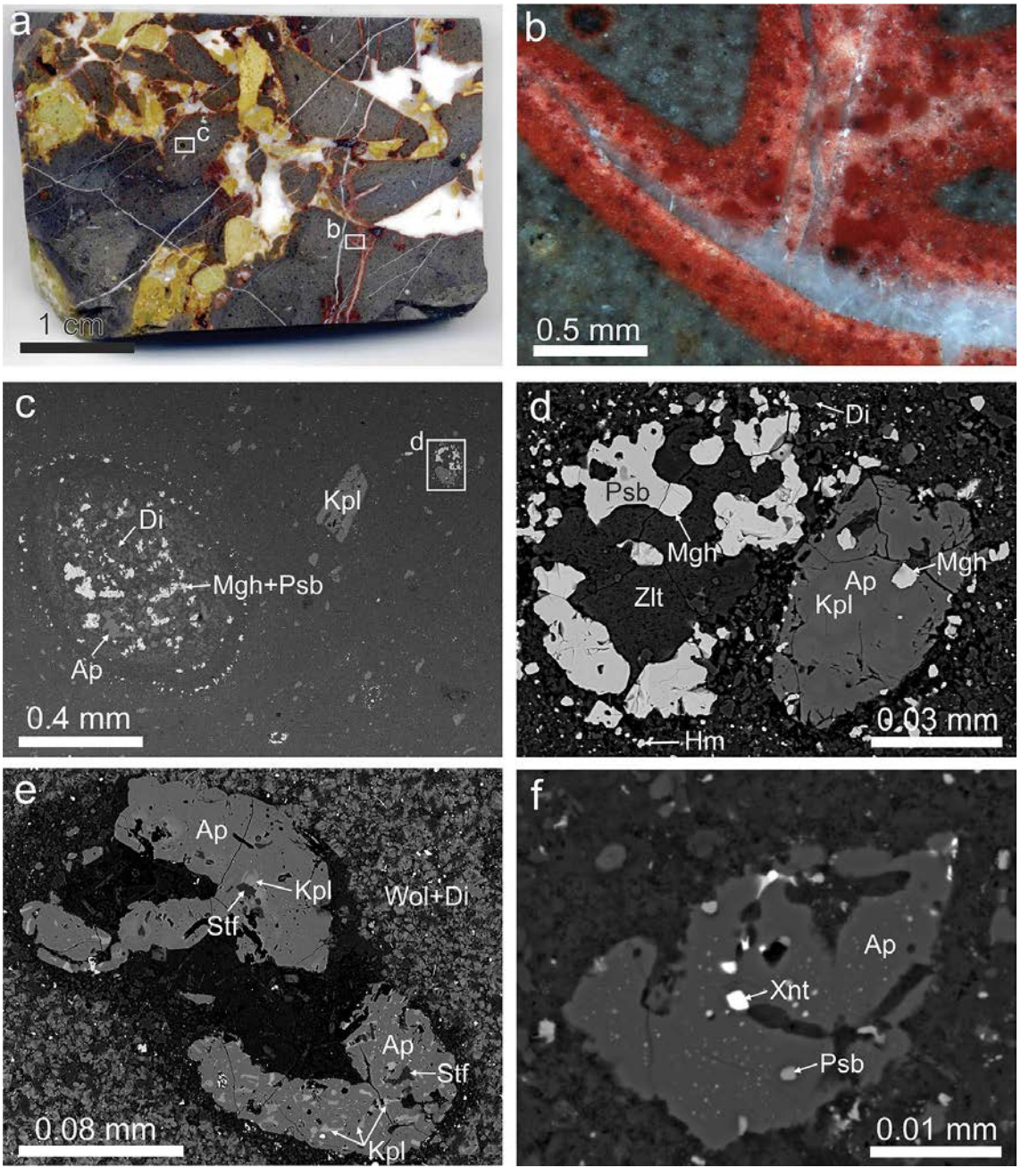

Figure 4. Keplerite-bearing assemblages in the paralava of the Hatrurim Basin. (**a**) Breccia-like rock composed of gray fragments with red thin rims, cemented by green-yellow fragments and white veinlets of secondary minerals. The fragments depicted in **b** and **c** are shown in frames. (**b**) The hematite-colored rim of gray breccia fragment. (**c**) Keplerite aggregates in the fine-grained diopside paralava. A fragment magnified in **d** is shown in frame. (**d**) A grain of keplerite intergrown with fluorapatite. (**e**) Stanfieldite and *REE*-bearing keplerite in fluorapatite. (**f**) Xenotime inclusions in fluorapatite. Mgh = maghemite; Di = diopside; Psb = pseudobrookite; Ap = fluorapatite; Kpl = keplerite; Hm = hematite; Zlt = zeolites; Stf = stanfieldite; Wol = wollastonite; Xnt = xenotime-(Y). (Color online.)

the total (Mg+Fe) content in type keplerite substantially exceeds the unity (in apfu) (Table 2), there must be another structural position capable of accommodating the observed excess of Fe^{2+}.

The [BO_6] polyhedron [denoted as the CaIIA site in the earlier works (e.g., Calvo and Gopal 1975; Dowty 1977)] has a shape of apex-truncated trigonal pyramid slightly twisted about the *c*-axis (Figs. 5 and 6a). In the anhydrous members of the whitlockite group, the *B*-site is partially or fully occupied by either Ca^{2+} or Na^{+} and shares a common face with the [$P(1)O_4$] tetrahedron (Fig. 6a). In the hydrogen-bearing members, the [$P(1)O_4$] tetrahedron is inverted along the *c*-axis, being tied up with three [$P(2)O_4$] tetrahedra via the hydrogen atom and the system of

TABLE 3. Chemical composition (wt%) of keplerite and associated phosphates from the pyrometamorphic hornfels of the Hatrurim basin

Phase number[a]	1	2	3	4	5	6
No. of points	3	1	10	4	2	6
CaO	48.39	46.64	45.61	42.22	23.20	54.66
SrO	–[b]	–	0.19	–	0.32	–
BaO	–	–	–	–	0.15	–
Na_2O	0.86	0.68	2.72	–	0.09	–
K_2O	–	–	0.12	–	–	–
MgO	3.73	3.72	3.50	3.50	23.67	0.56
MnO	–	–	–	–	0.13	0.06
FeO	–	0.65	0.15	0.35	3.11	0.20
Al_2O_3	–	–	–	0.05	–	–
Y_2O_3	–	0.76	0.43	3.75	–	–
La_2O_3	–	0.53	0.22	1.97	–	–
Ce_2O_3	–	0.27	–	1.27	–	–
Pr_2O_3	–	–	–	0.40	–	–
Nd_2O_3	–	0.43	0.24	1.93	–	–
Sm_2O_3	–	–	0.00	0.30	–	–
P_2O_5	45.85	45.25	45.12	43.54	49.52	42.04
V_2O_5	–	0.19	–	–	0.09	0.08
SiO_2	–	0.12	0.07	0.21	–	0.09
SO_3	–	0.19	0.24	0.30	0.26	0.07
F	tr[b]	tr	tr	tr	tr	3.82
$–O=F_2$						1.62
Total	98.83	99.43	98.61	98.79	100.54	99.96

[a] 1 = isolated keplerite grain, $Ca_{9.00}(Ca_{0.35}Na_{0.30})Mg_{1.00}(PO_4)_7$; 2 = keplerite intergrown with fluorapatite (Fig. 3d), $(Ca_{8.74}\textit{REE}_{0.16}Mg_{0.10})_{9.00}(Ca_{0.30}Na_{0.24})_{0.54}(Mg_{0.90}Fe^{2+}_{0.10})_{1.00}[(PO_4)_{6.93}(SO_4)_{0.03}(SiO_4)_{0.02}(VO_4)_{0.02}]_7$; 3 = merrilite, $(Ca_{8.87}\textit{REE}_{0.07}Na_{0.04}Sr_{0.02})_{9.00}(Na_{0.92}K_{0.03})_{0.95}(Mg_{0.95}Ca_{0.03}Fe^{2+}_{0.02})_{1.00}[(PO_4)_{6.96}(SO_4)_{0.03}(SiO_4)_{0.01}]_7$; 4 = "*REE*-merrilite," $(Ca_{8.18}\textit{REE}_{0.78}Mg_{0.04})_{9.00}Ca_{0.11}(Mg_{0.94}Fe^{3+}_{0.05}Al_{0.01})_{1.00}[(PO_4)_{6.92}(SO_4)_{0.04}(SiO_4)_{0.04}]_7$; 5 = stanfieldite, $(Ca_{6.88}Na_{0.05}Sr_{0.05}Ba_{0.02})_{7.00}(Mg_{1.04}Fe^{2+}_{0.74}Ca_{0.19}Mn^{2+}_{0.03})_{2.00}Mg_{9.00}[(PO_4)_{11.93}(SO_4)_{0.05}(VO_4)_{0.02}]_{12}$; 6 = fluorapatite from the intergrowth with keplerite (Fig. 3d), $(Ca_{4.91}Mg_{0.07}Fe^{2+}_{0.02})_{5.00}[(PO_4)_{2.98}(SiO_4)_{0.01}(SO_4)_{0.01}]_3F_{1.01}$.

[b] The dash means below detection limit; tr = traces.

hydrogen bonds (Fig. 6b) (e.g., Belik et al. 2003). Consequently, the *B*-site in the hydrogen-bearing whitlockite-group minerals is not vacant, but it is occupied by the P-O pair of $[P(1')O_4]$ and the H atom(s) (Fig. 6b). Consequently, the location of the $[P(1)O_4]$ tetrahedron relative to the truncated apex of the *B*-site allows structural distinction between the anhydrous and hydrous members of the whitlockite group (Table 1). In particular, the attachment of $[PO_4]$ tetrahedron to the truncated apex of the *B*-site (Fig. 6a) unambiguously provides evidence that keplerite from Marjalahti does not contain hydrogen. The freely refined site scattering factor of the *B*-site in keplerite is equal to 9.90 electron units that well corresponds to the mean atomic number of 11.80 derived from EMPA results (Tables 2 and 4). The latter gives the total Ca content of 9.33 apfu (Table 2) that, after subtraction of 9 Ca atoms residing in the $[AO_8]$ polyhedra, leaves 0.33 Ca atoms at the *B*-site. It should be noted, however, that due to the methodology of chemical calculations, the *B*-site population is a residual value, which accumulates all the analytical errors emerging in the course of EMPA (e.g., Shearer et al. 2015). The standard uncertainty of Ca determinations by electron microprobe is in the order of ~1–1.3 relative percent (e.g., Jolliff et al. 2006) that corresponds to 0.05–0.06 Ca apfu and thus yields 0.33(3) Ca apfu residing at the *B*-site. Therefore, there is still enough vacant space at the *B*-site (0.67 apfu) to accommodate other cations. Consequently, the observed excess of (Fe+Mg) in the Marjalahti mineral [Buseck and Holdsworth (1977) and our data (Table 2)] might indicate that Fe^{2+} in the holotype keplerite is incorporated in the *B*-site. This suggestion agrees well with the sixfold coordination of the *B*-site, contrary to the eightfold one of $[AO_8]$ polyhedra, and supported by previous reports on the same type of *B*-site substitutions in

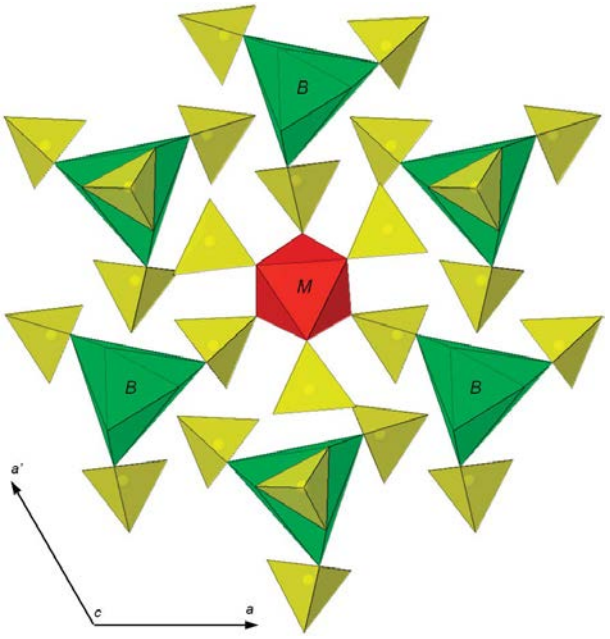

FIGURE 5. The arrangement of species-defining $[MO_6]$ octahedra (red) and $[BO_6]$ polyhedra (green) in the crystal structure of keplerite. Yellow: $[PO_4]$ tetrahedra. The $[AO_8]$ polyhedra are hidden for clarity. A slice along the plane parallel to (0001). (Color online.)

TABLE 4. Site populations and bond lengths for the *M* and *B* sites of keplerite and merrillite

Meteorite	Marjalahti	Angra Dos Reis	Suizhou	Brahin
Mineral[a]	Keplerite	Keplerite	Merrillite	Merrillite
	[1]	[2]	[3]	[4]
d(*M*–O6) (Å)	2.065(6)	2.078	2.070(2)	2.069(3)
d(*M*–O9) (Å)	2.093(6)	2.116	2.089(2)	2.091(3)
Mean *d*(*M*–O) (Å)	2.079	2.097	2.080	2.080
Site population (structure)	$Mg_{1.00}$[b]	$Mg_{0.78}Fe_{0.22}$	$Mg_{0.95}Fe_{0.05}$	$Mg_{1.00}$[b]
Site population (EMPA)	$Mg_{1.04}$	$Mg_{0.76}Fe_{0.19}$	$Mg_{0.95}Fe_{0.06}$	$Mg_{0.98}Fe_{0.01}$
d(*B*–O2) (Å)	2.790(9)	2.838	2.839(3)	2.848(5)
d(*B*–O3) (Å)	2.442(7)	2.442	2.411(2)	2.418(3)
Mean *d*(*X*–O) (Å)	2.616	2.640	2.625	2.633
Site population (structure)	$Ca_{0.33}Fe_{0.20}$[c]	$Ca_{0.55(1)}$	$Na_{1.00}$[d]	$Na_{1.00}$[d]
Site scattering factor (*e*)	9.90[e]	11.00[e]	11.00[d]	11.00[d]
Site population (EMPA)	$Ca_{0.33}Fe_{0.20}$	$Ca_{0.52}Na_{0.24}$	$Na_{0.98}$	$Na_{1.00}$
Mean *Z* (EMPA) (*e*)	11.80	13.04	10.78	11.00

[a] References: [1] this work, holotype specimen; [2] Dowty (1977); [3] Xie et al. (2015); [4] Britvin et al. (2016).

[b] Refined Fe content lies within 2σ error.

[c] Site population was fixed according to EMPA results.

[d] Not refined.

[e] Freely refined electron density assuming Ca X-ray scattering curve.

whitlockite-related phosphates (Schroeder et al. 1977; Britvin et al. 1991; Belik et al. 2003). The final structural refinement was carried out assuming a fixed $(Ca_{0.33}Fe_{0.20})$ *B*-site population perfectly converged (see the attached Online Materials[1] CIF file), confirming the correctness of the chemical formula determined from electron microprobe data.

Raman spectroscopy

The Raman spectrum of the holotype keplerite from the Marjalahti pallasite is shown in Figure 7 in comparison with the spectra of merrillite and ferromerrillite whose crystal structures

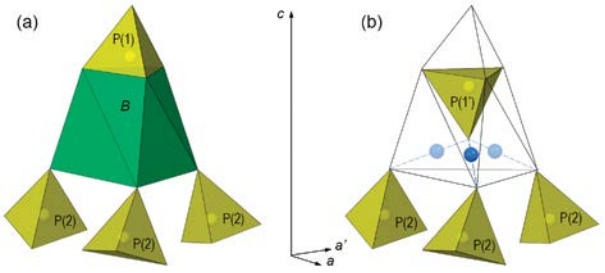

Figure 6. *B*-site environment in the structure of keplerite, $Ca_9Ca_{1/2}Mg(PO_4)_7$ (this work) and whitlockite-type $Ca_9FeD(PO_4)_7$ (Belik et al. 2003). (**a**) Keplerite (merrillite type): the *B* site is half-occupied by Ca^{2+}, and the hydrogen-free tetrahedron $[P(1)O_4]$ shares a common face with the apex-truncated trigonal pyramid $[BO_6]$. (2) $Ca_9FeD(PO_4)_7$: the *B* site is devoid of cations but occupied by a P-O pair of an inverted $[P(1')O_4]$ tetrahedron. The apexes of four $[PO_4]$ tetrahedra are tied together by the triply split proton (deuteron) (blue) via a system of hydrogen bonds (dashed lines). (Color online.)

were reported previously (Britvin et al. 2016). The absence of the band at 923 cm^{-1} demonstrates the lack of hydrogen phosphate groups (Jolliff et al. 1996), in accordance with the results of the structure refinement. All three minerals exhibit similar sets of Raman bands between 400 and 1080 cm^{-1} related to vibration modes of $[PO_4]$ tetrahedra (de Aza et al. 1997; Kovyazina et al. 2004; Jolliff et al. 2006) (Table 5). However, the strongest stretching vibration modes at 950–970 cm^{-1} in the spectrum of keplerite have a complex structure that is not observed in the spectra of merrillite and ferromerrillite (Fig. 8). The profile deconvolution (Lorenz shape approximation) gives in total 6 bands with the following fitted parameters [wavenumber (relative intensity, FWHM, cm^{-1})]: 950 (31, 6.7); 954 (35, 6.2); 958 (12. 7.6); 962 (10, 6.3); 968 (19, 6.3); and 971 (59, 5.3). The bands at 954 and 971 cm^{-1} coincide with the commonly observed ν_1 modes in the spectra of merrillite (e.g., Jolliff et al. 2006; Xie et al. 2015). However, to the best of our knowledge, the visually resolved shoulders at 950 and 958 cm^{-1} were not reported previously. These bands were observed in the Raman spectra of five different keplerite grains and thus are neither the artifacts nor phenomena related to the crystal orientation. The most likely explanation for their emergence is the local distortions in $[P(1)O_4]$ and $[P(2)O_4]$ tetrahedra adjoining the statistically half-occupied *B*-site (Fig. 6). The Raman spectra of terrestrial keplerite (Online Materials[1] Fig. OM1) are close to the spectra of minerals of the merrillite subgroup (Jolliff et al. 2006; Xie et al. 2015), bearing a characteristic duplet at 956–958 and 973–974 cm^{-1}.

Discussion

The origin of keplerite

The formation conditions of keplerite, $Ca_9(Ca_{0.5}\square_{0.5})Mg(PO_4)_7$ require the complete lack of Na and water in the mineral system. The presence of Na facilitates crystallization of intermediate merrillite-keplerite phases, whereas an aqueous medium can result in the emergence of whitlockite, $Ca_9Mg(PO_3OH)(PO_4)_6$. Accumulation of even traces of Na in the residual melts of pallasite meteorites leads to the emergence of merrillite—the sole Na-bearing phase in pallasites (Buseck and Holdsworth 1977). However, keplerite was discovered in another type of pallasite assemblages—in the orthopyroxene-troilite symplectites (Fig. 1) (Buseck 1977; Buseck and Holdsworth 1977). The two-phase composition and vermicular textures of these intergrowths are the same as of symplectites reported in acapulcoites (El Goresy et al. 2005; Folco et al. 2006), howardites (Patzer and McSween 2012), and brachinites (Goodrich et al. 2017). Although the above authors agree that the symplectites represent the quenched sulfide-silicate melts, the nature of an event(s) responsible for their formation is a matter of debate. Concerning the Marjalahti symplectites described herein, the apparent evidence is that they were formed prior to the shock event that caused the emergence of the Neumann bands (Figs. 1 and 2); otherwise the latter would be annealed during the heating process. However, the Neumann bands could be produced at the latest stage, upon the collision of the meteorite with the granite outcrop, as the projectile velocity

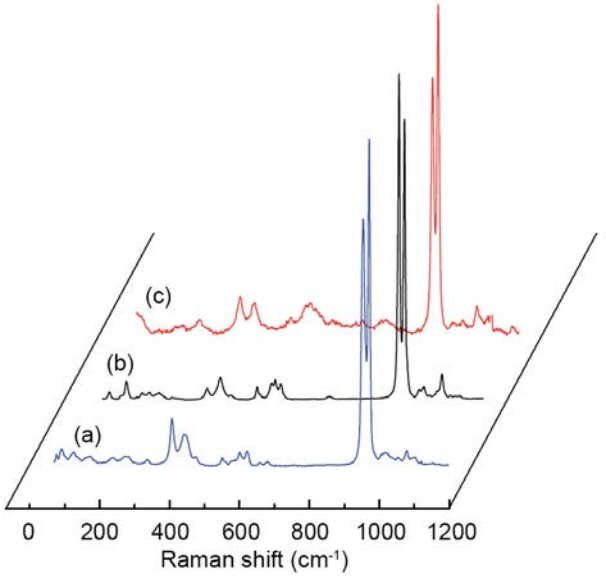

Figure 7. Raman spectra of (**a**) keplerite (the Marjalahti pallasite), (**b**) merrillite (the Brahin pallasite), and (**c**) ferromerrillite (the Los Angeles shergottite). The spectra (**b** and **c**) are shifted along the *x*-axis with the relative offset of 100 cm^{-1}. (Color online.)

Table 5. Frequencies of (PO_4) vibration modes (cm^{-1}) in the Raman spectra of keplerite, merrillite, and ferromerrillite

Mineral Meteorite Assignment[a]	Keplerite Marjalahti	Merrillite Brahin	Ferromerrillite Los Angeles
ν_2 (δ_s)	407	409	403
	442	446	445
ν_4 (δ_{as})	551	551	548
		593	591
	601	603	606
	622	618	620
		756	752
ν_1 (ν_s)	950[b]		
	954	957	954
	958[b]		
	971	973	970
ν_3 (ν_{as})	1016	1015	1012
	1078	1080	1080

[a] Band assignments according to de Aza et al. (1997); Kovyazina et al. (2004).
[b] Only visually resolved shoulders are listed (see Fig. 7).

was obviously sufficient for that (e.g., Uhlig 1955; Beck 2011). An interesting insight can be inferred from the results of a fission-track dating of the so-called "whitlockite" from Marjalahti (Pellas et al. 1983; Bondar and Perelygin 2005). Because neither Buseck and Holdsworth (1977) nor our study revealed the occurrence of merrillite in Marjalahti, one can suppose that the Na-free "whitlockite" used for the fission-track analysis was in fact represented by keplerite. As a result, keplerite and symplectites could have an age of ~4.3 Ga (Bondar and Perelygin 2005) and hence be directly related to the early crystallization history of Marjalahti. In that case, one can rule out the hypothesis of atmospheric ablation-induced origin of Marjalahti symplectites, such as that proposed for the similar Acapulco assemblages (El Goresy et al. 2005). It is important that the Mg-number of orthopyroxene in the symplectites from the Marjalahti pallasite is the same as of adjacent olivine crystals not affected by melting (Mg# = 88). Therefore, it is unlikely that the parent melts of the Marjalahti symplectites were subjected to redox differentiation (e.g., Righter et al. 1990), and the system was apparently a chemically closed and equilibrated one. The microgranular texture of troilite adjacent to symplectites suggests that this troilite was partially fused and then transferred into silicate melt pockets. The main open question is the overall SiO_2 budget, as there was no external Si source assuming that orthopyroxene was produced from, and equilibrated with, olivine. The thermally induced breakdown of a hypothetical Si-rich, Ca- and P-bearing Mg-silicate could explain both symplectite formation and the emergence of residual keplerite. However, no minerals with the acceptable composition were so far encountered in pallasites.

In contrast to pallasites, the origin of keplerite in the angrite meteorites (e.g., Keil et al. 1976; Crozaz and McKay 1990) is clearly related to the general crystallization pathways of these basaltic systems, which were reviewed in detail by Keil (2012). The variations in Mg/Fe ratio result in the emergence of an isomorphous series between keplerite and its Fe^{2+}-dominant analog, matyhite (Hwang et al. 2019).

The formation of terrestrial keplerite in the pyrometamorphic paralavas of the Hatrurim Formation is related to the local geochemical "microenvironments" that produce the known mineral diversity of this unique rock complex. Mineral compositions of keplerite-bearing paralava indicates that the primary source rocks for these assemblages were the paralavas related to the so-called "olive unit," whose likely protolith lithologies were the marls of the Taqiye Formation of Paleocene age (Burg et al. 1999). The origin of keplerite-bearing assemblages is related to the high-temperature alteration processes of primary paralavas of the olive unit, which were accompanied by brecciation of the rocks and the emergence of new generations of paralavas (Fig. 4a). Accessory fluorapatite is a primary mineral in these paralavas, and keplerite was likely formed as a product of thermally induced defluorination of fluorapatite (Figs. 4c and 4d). Where the latter was stuffed with the inclusions of xenotime and monazite, it was transformed into keplerite having high-*REE* contents.

The association of keplerite with merrillite, "*REE*-merrillite" and stanfieldite (Table 3) suggests the temperature conditions that governed the formation of these phosphate assemblages were similar to those encountered during the formation of meteorites and lunar rocks.

Keplerite position in the whitlockite group and the Na#

The crystal structure of whitlockite and related minerals bear three eightfold-coordinated [AO$_8$] polyhedra, which in total account for 9 Ca atoms per $A_9BM(PO_3X)_4(PO_4)_3$ formula unit that corresponds to almost 50 wt% CaO in the chemical composition. Geochemical conditions leave a little chance for any element to compete with Ca for the domination in the [AO$_8$] polyhedra; the sole exception is strontiowhitlockite, where A = Sr (Britvin et al. 1991). As a consequence, the mineral diversity within the whitlockite group is produced by (1) the interplay between substitutions at the B and M sites and (2) the attachment of acidic hydrogen(s) to $[PO_4]^{3-}$ tetrahedra to form hydrogen phosphate anion(s), $[HPO_4]^{2-} \equiv [PO_3OH]^{2-}$ (Table 1). Keplerite is related to its Na-counterpart, merrillite, by the heterovalent isomorphous substitution at the B-site of the crystal structure: $2Na^{+}$ (merrillite) $\rightarrow Ca^{2+} + \square$ (keplerite) and thus represents a distinct species (Hatert and Burke 2008; Bosi et al. 2019). The introduction of a unique name (rather than derivative from "merrillite") for keplerite highlights the

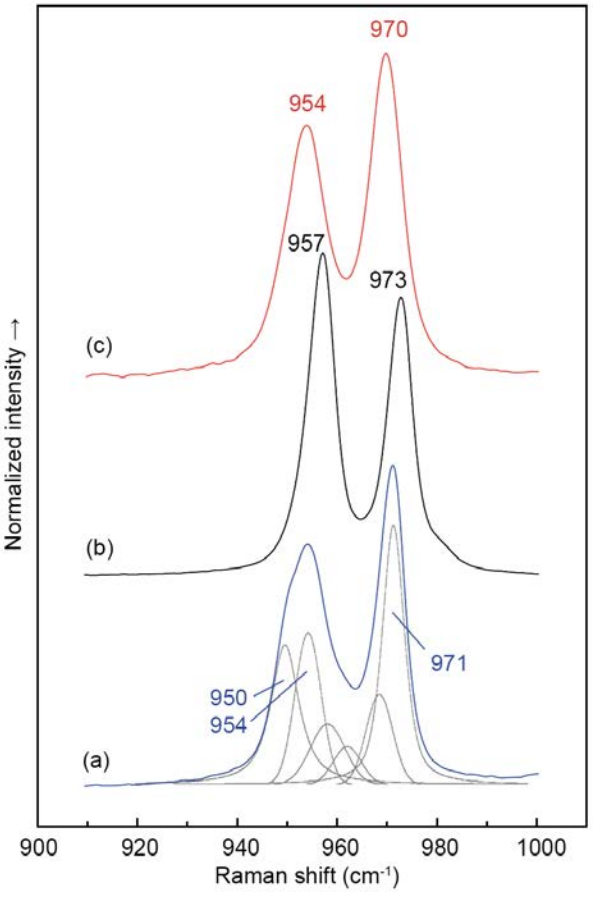

Figure 8. Detailed view of the Raman bands related to ν_1 (symmetric stretching) vibrations of [PO_4] tetrahedra. (**a**) Keplerite (the Marjalahti pallasite), with the band deconvolution curves; (**b**) merrillite (the Brahin pallasite); and (**c**) ferromerrillite (the Los Angeles shergottite). Note the visually resolved shoulders at 950 and 958 cm^{-1} in the spectrum of keplerite. (Color online.)

chemical and genetic difference between this mineral and other whitlockite-group species (Table 1). There is still substantial disorder in the literature concerning whitlockite-group minerals, in particular—intermixing of the names *merrillite* [an *anhydrous* $Ca_9NaMg(PO_4)_7$] and *whitlockite* [*water*-containing $Ca_9Mg(PO_3OH)(PO_4)_6$] (e.g., Sha 2000; Ionov et al. 2006; Pasek 2015; Keil and McCoy 2018; Carrillo-Sánchez et al. 2020). Meanwhile, the difference between water-containing and anhydrous minerals is not negligible but of paramount importance while dealing with reconstructions of geochemical/cosmochemical processes (Pernet-Fisher et al. 2014). The names like "Ca-merrillite" appear to add even more confusion, as merrillite itself, $Ca_9NaMg(PO_4)_7$, is a Ca-dominant mineral by definition, contrary to, e.g., strontiowhitlockite, $Sr_9Mg(PO_3OH)(PO_4)_6$ (Britvin et al. 1991). However, the general name merrillite is convenient for the use as a subgroup (≡ structure type) root name, like the commonly used root names tourmaline, garnet, plagioclase, etc. Because the minerals related to the join merrillite-keplerite are ubiquitous in the extraterrestrial matter, it appears to be convenient to quantify the role of Na in their composition (by analogy with, e.g., plagioclases). For this purpose, we herein propose the introduction of the Na-number (like the common Mg-number), formulated as 100×Na/(Na+Ca) in atomic amounts (Table 2). The merrillite end-member, $Ca_9NaMg(PO_4)_7$, has thus the Na-number = 10 whereas keplerite, $Ca_9(Ca_{0.5}\square_{0.5})Mg(PO_4)_7$, has the Na-number = 0.

Implications

The minerals belonging to the solid solutions merrillite-keplerite represent an important reservoir of phosphate phosphorus in the different kinds of solar system objects, from chondritic and achondritic meteorites, stony-irons, and irons to the lunar and martian rocks. The discovery of these minerals in Earth's mantle xenoliths (Ionov et al. 2006) and in the pyrometamorphic complex of the Hatrurim Formation opens new insights into their occurrence in the terrestrial rocks. Their crystal structures favor the selective accumulation of rare earth elements and actinides, making these minerals convenient targets for geological dating (Snape et al. 2016). The phase transformations of merrillite-type minerals into the high-pressure γ-$Ca_3(PO_4)_2$ polymorph (tuite) are sensitive indicators of impact events experienced by the parent celestial bodies (Xie et al. 2002). Therefore, revealing the new structural and genetic relationships between merrillite–keplerite minerals and associated phases would add more knowledge toward understanding the processes of solar system formation.

Acknowledgments

The authors are thankful to the curators of the Mining Museum, St. Petersburg Mining Institute, for providing meteorite samples. We are grateful to Associate Editor Fabrizio Nestola for the handling of the manuscript and to the Technical Editor for the correction of crystallographic data. The authors are indebted to the reviewers, Pietro Vignola and Ferdinando Bosi, who made valuable suggestions that substantially enhanced the contents of the article.

Funding

This research was supported by the Russian Science Foundation, Grant 18-17-00079 (the study of holotype, meteoritic keplerite), and by the National Science Centre (NCN) of Poland, grant no. 2016/23/B/ST10/00869 (the part related to terrestrial keplerite). We thank the X-ray Diffraction Centre and "Geomodel" Resource Centre of St. Petersburg State University for instrumental and computational support.

References cited

Adcock, C.T., Hausrath, E.M., Forster, P.M., Tschauner, O., and Sefein, K.J. (2014) Synthesis and characterization of the Mars-relevant phosphate minerals Fe and Mg-whitlockite and merrillite and a possible mechanism that maintains charge balance during whitlockite to merrillite transformation. American Mineralogist, 99, 1221–1232.

Beck, S.D., Nakasone, H., and Marr, K.W. (2011) Variations in recorded acoustic gunshot waveforms generated by small firearms. The Journal of the Acoustical Society of America, 129, 1748–1759.

Belik, A.A., Izumi, F., Stefanovich, S.Y., Lazoryak, B.I., and Oikawa, K. (2003) Chemical and structural properties of a whitlockite-like phosphate, $Ca_9FeD(PO_4)_7$. Chemistry of Materials, 15, 1399–1400.

Boesenberg, J.S., Delaney, G.S., and Hewins, R.H.J. (2012) A petrological and chemical reexamination of Main Group pallasite formation. Geochimica et Cosmochimica Acta, 89, 134–158.

Bondar, Y.V., and Perelygin, V.P. (2005) Fission-track analysis of meteorites: Dating of the Marjalahti pallasite. Radiation Measurements, 40, 522–527.

Bosi, F., Hatert, F., Hålenius, U., Pasero, M., Miyawaki, R., and Mills, S.J. (2019) On the application of the IMA-CNMNC dominant-valency rule to complex mineral compositions. Mineralogical Magazine, 83, 627–632.

Britvin, S.N., Pakhomovskii, Y.A., Bogdanova, A.N., and Skiba, V.I. (1991) Strontiowhitlockite, $Sr_9Mg(PO_3OH)(PO_4)_6$, a new mineral species from the Kovdor deposit, Kola Peninsula, U.S.S.R. Canadian Mineralogist, 29, 87–93.

Britvin, S.N., Murashko, M.N., Vapnik, Y., Polekhovsky, Y.S., and Krivovichev, S.V. (2015) Earth's phosphides in Levant and insights into the source of Archaean prebiotc phosphorus. Scientific Reports, 5, 8355.

Britvin, S.N., Krivovichev, S.V., and Armbruster, T. (2016) Ferromerrillite, $Ca_9NaFe^{2+}(PO_4)_7$, a new mineral from the martian meteorites, and some insights into merrillite-tuite transformation in shergottites. European Journal of Mineralogy, 28, 125–136.

Britvin, S.N., Krzhizhanovskaya, M.G., Bocharov, V.N., and Obolonskaya, E.V. (2020) Crystal chemistry of stanfieldite, $Ca_7M_2Mg_9(PO_4)_{12}$ (M = Ca, Mg, Fe^{2+}), a structural base of $Ca_3Mg_3(PO_4)_4$ phosphors. Crystals, 10, 464.

Burg, A., Kolodny, Ye., and Lyakhovsky, V. (1999) Hatrurim—2000: The "Mottled Zone" revisited, forty years later. Israel Journal of Earth Sciences, 48, 209–223.

Buseck, P.R. (1977) Pallasite meteorites—Mineralogy, petrology and geochemistry. Geochimica et Cosmochimica Acta, 41, 711–740.

Buseck, P.R., and Holdsworth, E. (1977) Phosphate minerals in pallasite meteorites. Mineralogical Magazine, 41, 91–102.

Calvo, C., and Gopal, R. (1975) The crystal structure of whitlockite from the Palermo Quarry. American Mineralogist, 60, 120–133.

Carrillo-Sánchez, J.D., Bones, D.L., Douglas, K.M., Flynn, G.J., Wirick, S., Fegley, B. Jr., Araki, T., Kaulich, B., and Plane, J.M.C. (2020) Injection of meteoric phosphorus into planetary atmospheres. Planetary and Space Science, 187, 104926.

Cooper, M.A., Hawthorne, F.C., Abdu, Y.A., Ball, N.A., Ramik, R.A., and Tait, K.T. (2013) Wopmayite, ideally $Ca_6Na_2Mn(PO_4)_3(PO_3OH)_4$, a new phosphate mineral from the Tanco Mine, Bernic Lake, Manitoba. Canadian Mineralogist, 51, 93–106.

Crozaz, G., and McKay, G. (1990) Rare earth elements in Angra dos Reis and Lewis Cliff 86010, two meteorites with similar but distinct magma evolutions. Earth and Planetary Science Letters, 97, 369–381.

de Aza, P.N., Santos, C., Pazo, A., de Aza, S., Cuscó, R., and Artús, L. (1997) Vibrational properties of calcium phosphate compounds. 1. Raman spectrum of β-tricalcium phosphate. Chemistry of Materials, 9, 912–915.

Dolomanov, O.V., Bourhis, L.J., Gildea, R.J., Howard, J.A., and Puschmann, H. (2009) OLEX2: A complete structure solution, refinement and analysis program. Journal of Applied Crystallography, 42, 339–341.

Dowty, E. (1977) Phosphate in Angra dos Reis: Structure and composition of the $Ca_3(PO_4)_2$ minerals. Earth and Planetary Science Letters, 35, 347–351.

El Goresy, A., Zinner, E., Pellas, P., and Caillet, C. (2005) A menagerie of graphite morphologies in the Acapulco meteorite with diverse carbon and nitrogen isotopic signatures: Implications for the evolution history of acapulcoite meteorites. Geochimica et Cosmochimica Acta, 69, 4535–4556.

Folco, L., D'Orazio, M., and Burroni, A. (2006) Frontier Mountain 93001: A coarse-grained, enstatite-augite-oligoclase-rich, igneous rock from the acapulcoite-lodranite parent asteroid. Meteoritics & Planetary Science, 41, 1183–1198.

Frondel, C. (1941) Whitlockite: A new calcium phosphate $Ca_3(PO_4)_2$. American Mineralogist, 26, 145–152.

——— (1943) Mineralogy of the calcium phosphates in insular phosphate rock. American Mineralogist, 28, 215–232.

Fuchs, L.H. (1962) Occurrence of whitlockite in chondritic meteorites. Science, 137, 425–426.

Galuskina, I.O., Vapnik, Y., Lazic, B., Armbruster, T., Murashko, M., and Galuskin, E.V. (2014) Harmunite $CaFe_2O_4$: A new mineral from the Jabel Harmun, West Bank, Palestinian Autonomy, Israel. American Mineralogist, 99, 965–975.

Galuskina, I.O., Galuskin, E.V., and Vapnik, Y.A. (2016) Terrestrial merrillite. 2nd European Mineralogical Conference. Plinius, 42, 563. Abstract.

Galuskin, E.V., Galuskina, I.O., Gfeller, F., Krüger, B., Kusz, J., Vapnik, Y., Dulski, M., and Dzierżanowski, P. (2016) Silicocarnotite, $Ca_5[(SiO_4)(PO_4)](PO_4)$, new "old" mineral from the Negev Desert, Israel, and the ternesite-silicocarnotite

solid solution: Indicators of high-temperature alteration of pyrometamorphic rocks of the Hatrurim Complex, Southern Levant. European Journal of Mineralogy, 28, 105–123.
Galuskin, E., Krüger, B., Galuskina, I., Krüger, H., Vapnik, Y., Wojdyla, J., and Murashko, M. (2018a) New mineral with modular structure derived from hatrurite from the pyrometamorphic rocks of the Hatrurim Complex: Ariegilatite, $BaCa_{12}(SiO_4)_4(PO_4)_2F_2O$, from Negev Desert, Israel. Minerals, 8, 109.
Galuskin, E.V., Krüger, B., Galuskina, I.O., Krüger, H., Vapnik, Y., Pauluhn, A., and Olieric, V. (2018b) Stracherite, $BaCa_6(SiO_4)_2[(PO_4)(CO_3)]F$, the first CO_3-bearing intercalated hexagonal antiperovskite from Negev Desert. American Mineralogist, 103, 1699–1706.
Geller, Y.I., Burg, A., Halicz, L., and Kolodny, Y. (2012) System closure during the combustion metamorphic "Mottled Zone" event. Chemical Geology, 334, 25–36.
Goodrich, C.A., Kita, N.T., Sutton, S.R., Wirick, S., and Gross, J. (2017) The Miller Range 090340 and 090206 meteorites: Identification of new brachinite-like achondrites with implications for the diversity and petrogenesis of the brachinite clan. Meteoritics & Planetary Science, 52, 949–978.
Gopal, R., and Calvo, C. (1972) Structural relationship of whitlockite and β-$Ca_3(PO_4)_2$. Nature Physical Science, 237, 30–32.
Grady, M.M. (2000) Catalogue of Meteorites. Cambridge University Press, New York.
Gross, H. (1977) The mineralogy of the Hatrurim Formation. Israel. Geological Survey of Israel Bulletin, 70, 1–80.
Hatert, F., and Burke, E.A.J. (2008) The IMA-CNMNC dominant-constituent rule revisited and extended. Canadian Mineralogist, 46, 717–728.
Hughes, J.M., Jolliff, B.L., and Gunter, M.E. (2006) The atomic arrangement of merrillite from the Fra Mauro Formation, Apollo 14 lunar mission: The first structure of merrillite from the Moon. American Mineralogist, 91, 1547–1552.
Hughes, J.M., Jolliff, B.L., and Rakovan, J. (2008) The crystal chemistry of whitlockite and merrillite and the dehydrogenation of whitlockite to merrillite. American Mineralogist, 93, 1300–1305.
Hwang, S.-L., Shen, P., Chu, H.-T., Yui, T.-F., Varela, M.E., and Iizuka, Y. (2019) New minerals tsangpoite $Ca_5(PO_4)_2(SiO_4)$ and matyhite $Ca_9(Ca_{0.5}\square_{0.5})Fe(PO_4)_7$ from the D'Orbigny angrite. Mineralogical Magazine, 83, 293–313.
Ionov, D.A., Hofmann, A.W., Merlet, C., Gurenko, A.A., Hellebrand, E., Montagnac, G., Gillet, P., and Prikhodko, V.S. (2006) Discovery of whitlockite in mantle xenoliths: Inferences for water- and halogen-poor fluids and trace element residence in the terrestrial upper mantle. Earth and Planetary Science Letters, 244, 201–217.
Jolliff, B.L., Freeman, J.J., and Wopenka, B. (1996) Structural comparison lunar, terrestrial, and synthetic whitlockite using laser Raman microprobe spectroscopy. Lunar and Planetary Science, XXII, 613–614. Abstract.
Jolliff, B.L., Hughes, J.M., Freeman, J.J., and Zeigler, R.A. (2006) Crystal chemistry of lunar merrillite and comparison to other meteoritic and planetary suites of whitlockite and merrillite. American Mineralogist, 91, 1583–1595.
Jones, R.H., McCubbin, F.M., Dreeland, L., Guan, Y.B., Burger, P.V., and Shearer, C.K. (2014) Phosphate minerals in LL chondrites: A record of the action of fluids during metamorphism on ordinary chondrite parent bodies. Geochimica et Cosmochimica Acta, 132, 120–140.
Jones, R.H., McCubbin, F.M., and Guan, Y. (2016) Phosphate minerals in the H group of ordinary chondrites, and fluid activity recorded by apatite heterogeneity in the Zag H3-6 regolith breccia. American Mineralogist, 101, 2452–2467.
Keil, K. (2012) Angrites, a small but diverse suite of ancient, silica-undersaturated volcanic-plutonic mafic meteorites, and the history of their parent asteroid. Geochemistry, 72, 191–218.
Keil, K., and McCoy, T.J. (2018) Acapulcoite-lodranite meteorites: Ultramafic asteroidal partial melt residues. Geochemistry, 78, 153–203.
Keil, K., Prinz, M., Hlava, P.F., Gomes, C.B., Curvello, W.S., Wasserburg, G.J., Tera, F., Papanastassiou, D.A., Huneke, J.C., Murali, A.V., and others (1976) Progress by the consorts of Angra dos Reis (The Adorables). Abstracts of Lunar and Planetary Science Conference, 7, 443–445.
Kepler, I. (1611) Strena seu de nive sexangula. Godefridum Tampach, Francofurti ad Moenum.
Khoury, H.N. (2020) High- and low-temperature mineral phases from the pyrometamorphic rocks, Jordan. Arabian Journal of Geosciences, 13, 734.
Kovyazina, S.A., Perelyaeva, L.A., Leonidova, O.N., Leonidov, I.A., and Ivanovskii, A.L. (2004) High-temperature Raman spectroscopy and phase transformations in phosphates and vanadates $Ca_{3-3x}Nd_{2x}(AO_4)_2$ (A = P, V; $0 \le x \le 0.14$). Crystallography Reports, 49, 211–214.
Krüger, B., Krüger, H., Galuskin, E.V., Galuskina, I.O., Vapnik, Y., Olieric, V., and Pauluhn, A. (2018) Aravaite, $Ba_2Ca_{18}(SiO_4)_6(PO_4)_3(CO_3)F_3O$: modular structure and disorder of a new mineral with single and triple antiperovskite layers. Acta Crystallographica, B74, 492–501.
Krüger, B., Galuskin, E.V., Galuskina, I.O., Krüger, H., and Vapnik, Y. (2019) Kahlenbergite, IMA 2018-247. CNMNC Newsletter. Mineralogical Magazine, 83, 479–493.
Lewis, J., and Jones, R.H. (2016) Phosphate and feldspar mineralogy of equilibrated L chondrites: The record of metasomatism during metamorphism in ordinary chondrite parent bodies. Meteoritics & Planetary Science, 51, 1886–1913.
Mandarino, J.A. (1981) The Gladstone-Dale relationship. IV. The compatibility concept and its application. Canadian Mineralogist, 19, 441–450.
McCubbin, F.M., and Jones, R.H. (2015) Extraterrestrial apatite: Planetary geochemistry to astrobiology. Elements, 11, 183–188.
Merrill, G.P. (1915) On the monticellite-like mineral in meteorites, and on oldhamite as a meteoric constituent. Proceedings of the National Academy of Sciences, 1, 302–308.
Moore, P.B. (1973) Bracelets and pinwheels: a topological-geometric approach to the calcium orthosilicates and alkali sulfate structures. American Mineralogist, 58, 32–42.
Novikov, I., Vapnik, Y., and Safonova, I. (2013) Mud volcano origin of the Mottled Zone, Southern Levant. Geoscience Frontiers, 4, 597–619.
Oxford Diffraction (2018) CrysAlisPro 171.40. Oxford Diffraction Ltd, Abingdon, England.
Pasek, M. (2015) Phosphorus as a lunar volatile. Icarus, 255, 18–23.
Patzer, A., and McSween, H.Y. (2012) Ordinary (mesostasis) and not-so-ordinary (symplectites) late-stage assemblages in howardites. Meteoritics & Planetary Science, 47, 1475–1490.
Pellas, P., Perron, C., Crozaz, G., Perelygin, V.P., and Stetsenko, S.G. (1983) Fission track age and cooling rate of the Marjalahti pallasite. Earth and Planetary Science Letters, 64, 319–326.
Pernet-Fisher, J.F., Howarth, G.H., Liu, Y., Chen, Y., and Taylor, L.A. (2014) Estimating the lunar mantle water budget from phosphates: Complications associated with silicate-liquid-immiscibility. Geochimica et Cosmochimica Acta, 144, 326–341.
Righter, K., Arculus, R.J., Paslick, C., and Delano, J.W. (1990) Electrochemical measurements and thermodynamic calculations of redox equilibria in pallasite meteorites—Implications for the eucrite parent body. Geochimica et Cosmochimica Acta, 54, 1803–1815.
Schroeder, L.W., Dickens, B., and Brown, W.E. (1977) Crystallographic studies of the role of Mg as a stabilizing impurity in beta-$Ca_3(PO_4)_2$. II. Refinement of Mg-containing beta-$Ca_3(PO_4)_2$. Journal of Solid State Chemistry, 22, 253–262.
Sha, L.K. (2000) Whitlockite solubility in silicate melts: Some insights into lunar and planetary evolution. Geochimica et Cosmochimica Acta, 64, 3217–3236.
Shearer, C.K., Burger, P.V., Papike, J.J., McCubbin, F.M., and Bell, A.S. (2015) Crystal chemistry of merrillite from martian meteorites: Mineralogical recorders of magmatic processes and planetary differentiation. Meteoritics & Planetary Science, 50, 649–673.
Sheldrick, G.M. (2015) Crystal structure refinement with *SHELXL*. Acta Crystallographica, C71, 3–8.
Snape, J.F., Nemchin, A.A., Grange, M.L., Bellucci, J.J., Thiessen, F., and Whitehouse, M.J. (2016) Phosphate ages in Apollo 14 breccias: Resolving multiple impact events with high precision U–Pb SIMS analyses. Geochimica et Cosmochimica Acta, 174, 13–29.
Sokol, E.V., Kokh, S.N., Sharygin, V.V., Danilovsky, V.A., Seryotkin, Y.V., Liferovich, R., Deviatiiarova, A.S., Nigmatulina, E.N., and Karmanov, N.S. (2019) Mineralogical diversity of Ca_2SiO_4-bearing combustion metamorphic rocks in the Hatrurim Basin: Implications for storage and partitioning of elements in oil shale clinkering. Minerals, 9, 465.
Uhlig, H.H. (1955) Contribution of metallurgy to the origin of meteorites Part II—The significance of Neumann bands in meteorites. Geochimica et Cosmochimica Acta, 7, 34–42.
Van Schmus, W.R., and Ribbe, P.H. (1969) Composition of phosphate minerals in ordinary chondrites. Geochimica et Cosmochimica Acta, 33, 637–640.
Vapnik, Y., Sharygin, V.V., Sokol, E.V., and Shagam, R. (2007) Paralavas in a combustion metamorphic complex: Hatrurim Basin, Israel. The Geological Society of America, Reviews in Engineering Geology, 18, 133–153.
Wang, L., and Nancollas, G.H. (2008) Calcium orthophosphates: crystallization and dissolution. Chemical Reviews, 108, 4628–4669.
Ward, D., Bischoff, A., Roszjar, J., Berndt, J., and Whitehouse, M.J. (2017) Trace element inventory of meteoritic Ca-phosphates. American Mineralogist, 102, 1856–1880.
Witzke, T., Phillips, B.L., Woerner, W., Countinho, J.M.V., Färber, G., and Contreira Filho, R.R. (2015) Hedegaardite, IMA 2014-069. CNMNC Newsletter No. 23. Mineralogical Magazine, 79, 51–58.
Xie, X., Minitti, M.E., Chen, M., Mao, H.K., Wang, D., Shu, J., and Fei, Y. (2002) Natural high-pressure polymorph of merrillite in the shock vein of the Suizhou meteorite. Geochimica et Cosmochimica Acta, 66, 2439–2444.
Xie, X., Yang, H., Gu, X., and Downs, R.T. (2015) Chemical composition and crystal structure of merrillite from the Suizhou meteorite. American Mineralogist, 100, 2753–2756.

Manuscript received September 29, 2020
Manuscript accepted December 21, 2020
Manuscript handled by Fabrizio Nestola

Endnote:

[1]Deposit item AM-21-127834, Online Materials. Deposit items are free to all readers and found on the MSA website, via the specific issue's Table of Contents (go to http://www.minsocam.org/MSA/AmMin/TOC/2021/Dec2021_data/Dec2021_data.html). The CIF has been peer reviewed by our Technical Editors.